

Simple Models for Aspects of IFE Shock Mitigation

Jeff Lawrence and Lalit Chhabildas
Sandia National Laboratories



12 – 16 November 2006
Albuquerque, New Mexico

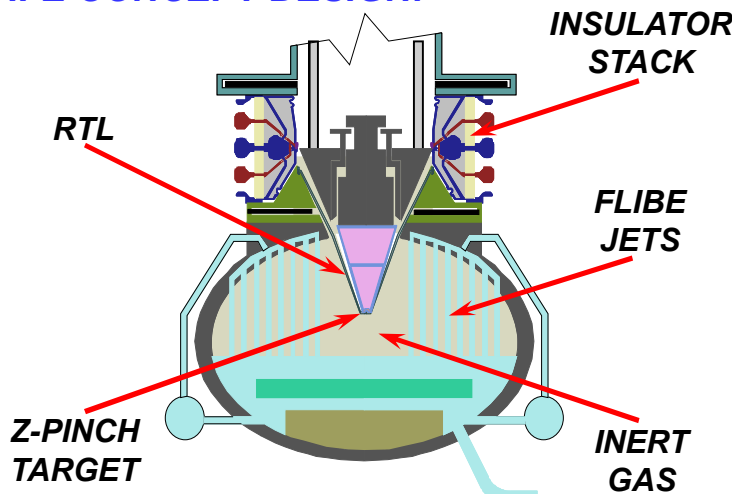


Sandia is a multiprogram laboratory operated by Sandia Corporation, a Lockheed Martin Company,
for the United States Department of Energy's National Nuclear Security Administration under contract DE-AC04-94AL85000.

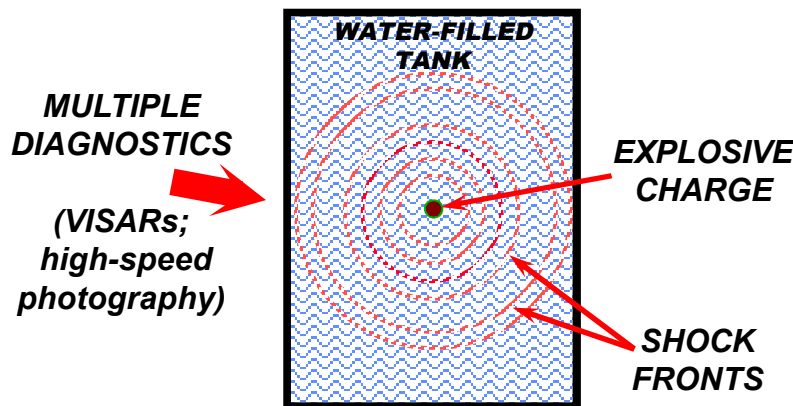


Any IFE power-plant design (e.g., ZP3) will need shock mitigation to maintain system integrity.

IFE CONCEPT DESIGN:



VALIDATION EXPs:

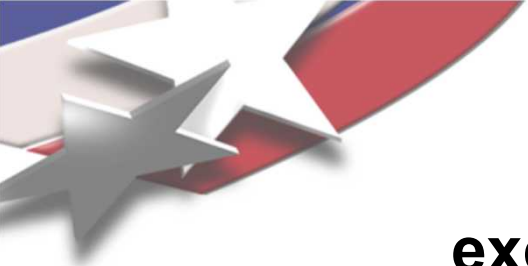


- Major goals for present effort:
 - > Provide initial estimates for dynamic loads generated by large x-ray pulses
 - > Suggest simple approaches to study mitigation techniques
- Approach:
 - > Run simple hydrocode analyses to rank importance of various phenomena (initial study used water in preparation for possible model validation experiments using high explosives)
 - > Employ analytic models to bound important parameters and loading levels



Preliminary analysis on energy-driven shock attenuation in water used the WONDY code.

- Calculations were all performed with the one-dimensional Lagrangian hydrocode WONDY:
 - > Both planar and cylindrical symmetries were used.
 - > The numerical mesh consisted of 3,050 zones representing: 1) the source region (50 zones); and 2) an additional 80 source-region thicknesses (3,000 zones).
 - > Typical runs extend to 50,000 time cycles or more.
 - > Calculations run in a few minutes or less on a typical laptop.
- The nominal calculation involved the following base configuration:
 - > Energy was deposited in the axially-located source region of thickness (or radius) 1 cm.
 - > The “initial load” (or energy deposition) in the source region was $p \approx 1 \text{ Mbar}$ ($\mathcal{E}_0 = 100 \text{ kJ/g}$, $\rho_0 \approx 1 \text{ g/cm}^3$, $\gamma_0 = 1$).
 - > Energy was deposited over 1 ns, which is “short” compared to the shock transit time across the source region ($\sim 0.7 \mu\text{s}$).
 - > Water was represented by the U_s/U_p Hugoniot, $U_s = 1.48 + 1.77 U_p$ (km/s); as well as by $\rho_0 = 0.9982 \text{ g/cm}^3$ for the density, and $\gamma_0 = 1.0$ for the Grüneisen parameter.

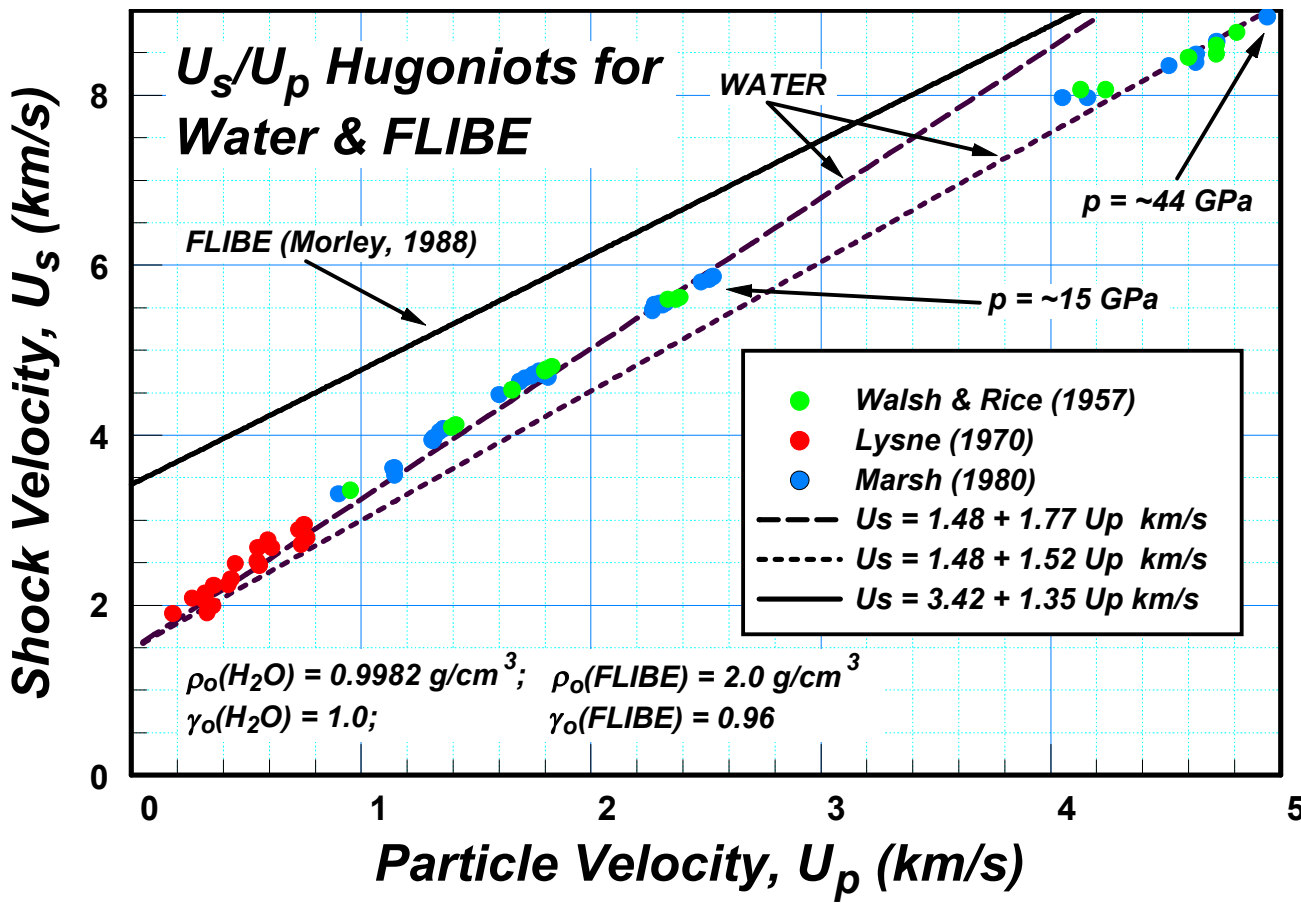


We examined various excursions from the nominal configuration.

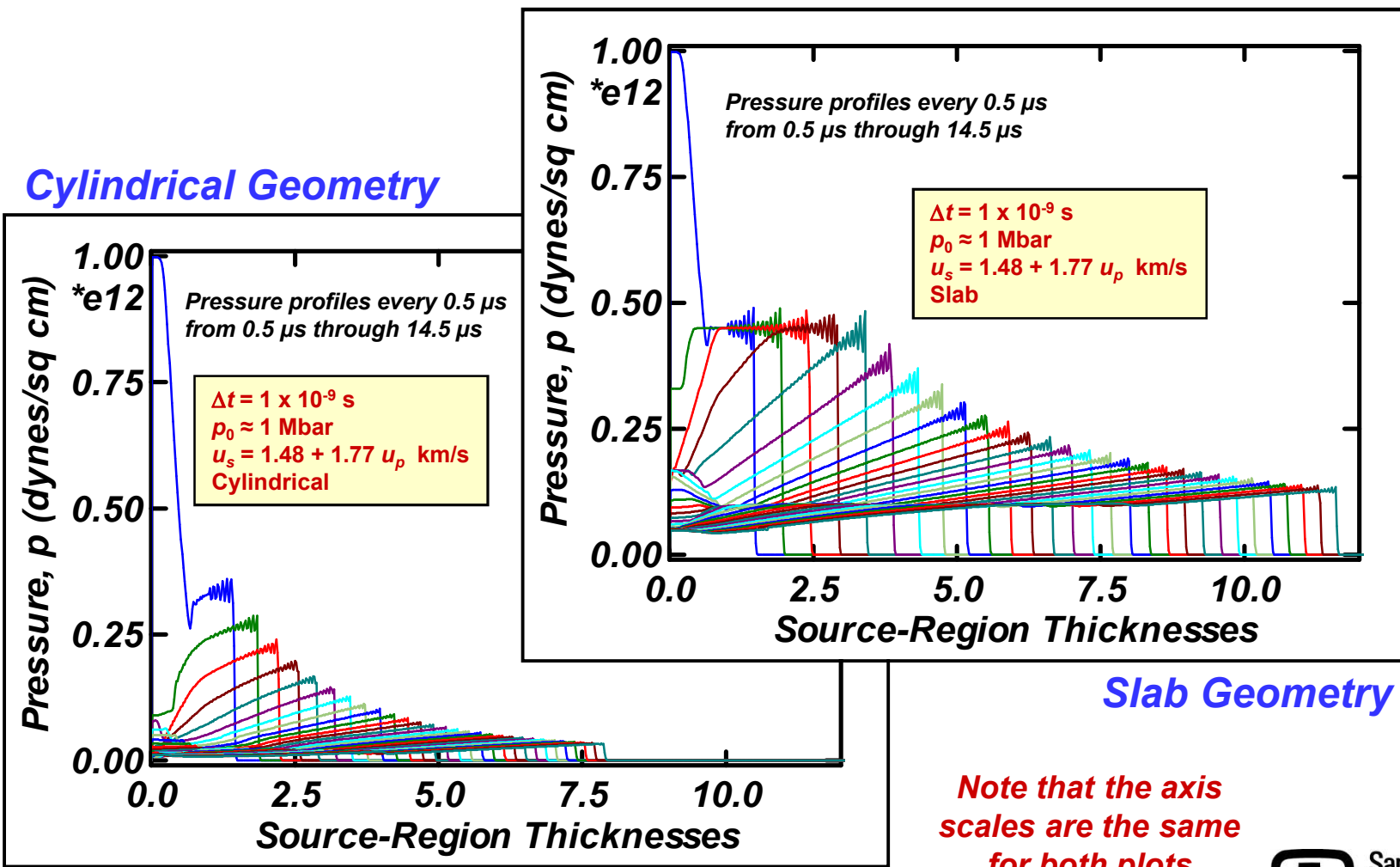
- Computational variations involved:
 - > Comparison of slab and cylindrical geometries;
 - > Energy source durations that were short, similar, and long compared to the shock transit times across the source region –
 - $\Delta t = 1$ ns (short)
 - $\Delta t = 1$ μ s (similar)
 - $\Delta t = 100$ μ s (long)
 - > Low- and high-pressure, and polynomial equations of state (EOSs) –
 - Low-pressure EOS: $U_s = 1.48 + 1.77 U_p$ km/s
 - High-pressure EOS: $U_s = 1.48 + 1.52 U_p$ km/s
 - Polynomial EOS ($\eta = 1 - \rho_0/\rho$): $p = 2.19 \eta (1 - 6.81 \eta + 31.7 \eta^2 + 91.6 \eta^3 + 129 \eta^4)$ GPa
 - > Changes in the “initial load” to show importance of EOS nonlinearities –
 - $p_0 \approx 1$ Mbar (large): $\mathcal{E}_0 = 100$ kJ/g, with $\rho_0 \approx 1$ g/cm³, $\gamma_0 = 1$
 - $p_0 \approx 1$ kbar (small): $\mathcal{E}_0 = 100$ J/g, with $\rho_0 \approx 1$ g/cm³, $\gamma_0 = 1$
 - > Additional calculations that employed a Z-type $p(t)$ loading.
- Detailed results are plotted in terms of pressure histories at evenly spaced Lagrangian points in the water outside the source region. Illustrative pressure profiles at evenly spaced times are also given to show the early-time behavior of the configurations. Normalized peak-pressure data are tabulated.



The equations of state for relevant materials can be described by linear fits on the U_s/U_p plane.

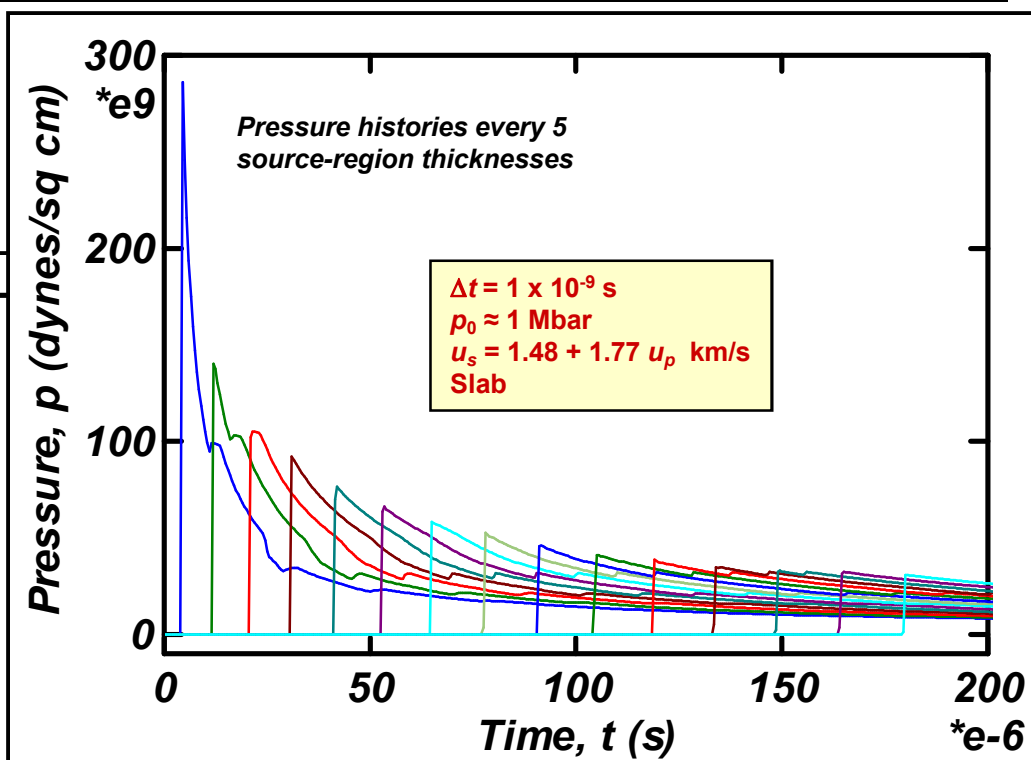
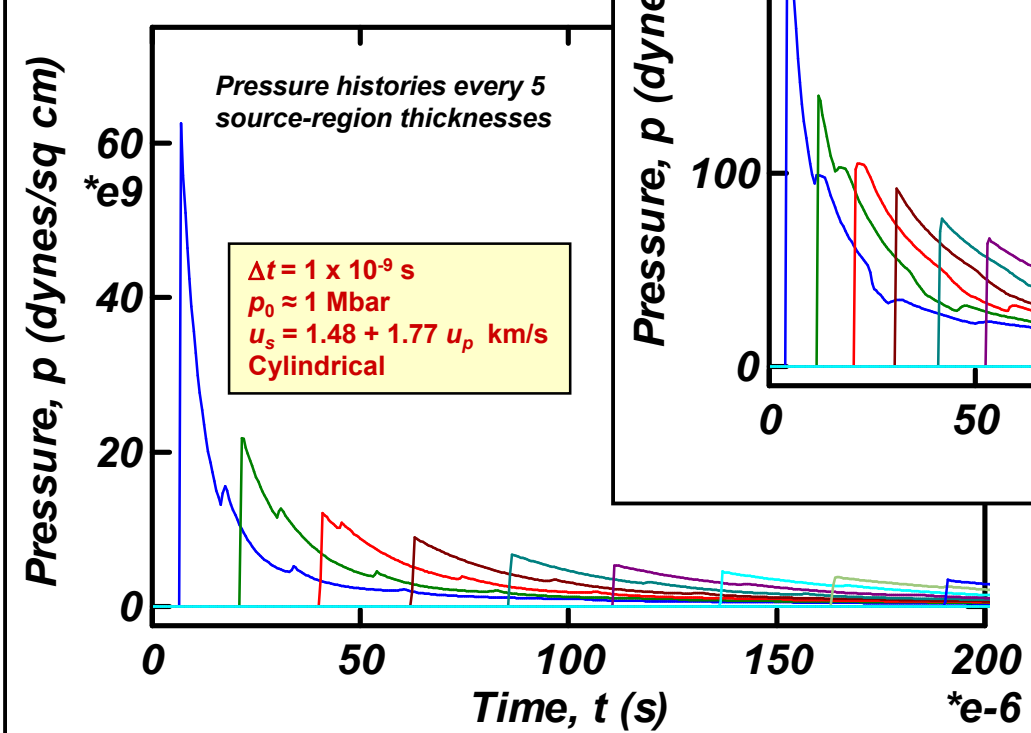


Early-time pressure profiles show the large differences between slab and cylindrical geometries.



Later-time results show even greater effects in attenuation and propagation velocities.

Cylindrical Geometry



Slab Geometry

Note the factor of 4 difference in the pressure axes



Sandia
National
Laboratories



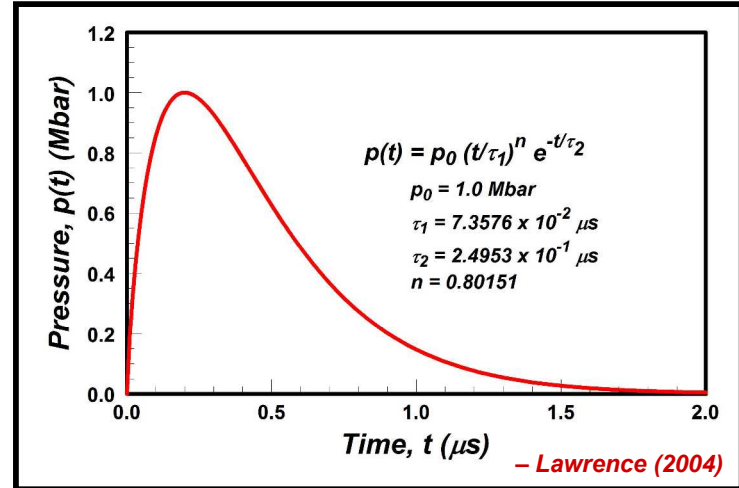
Pressure attenuation for energy-driven shock loading in water shows various dependencies . . .

<i>Driving Pressure</i>	<i>Energy Pulse Width</i>	<i>Equation of State</i>	<i>Lagrangian Position</i>	<i>Slab Geometry</i> *	<i>Cylindrical Geometry</i> *
1 Mbar	1 ns	Lo-Pressure	10 cm	0.148	0.023
			75 cm	0.031	0.0023
1 Mbar	1 ns	Hi-Pressure	10 cm	0.146	0.023
			75 cm	0.030	0.0020
1 Mbar	1 ns	Polynomial $p(\eta)$	10 cm	0.170	0.020
			75 cm	0.028	0.0013
1 Mbar	1 μ s	Lo-Pressure	10 cm	0.151	0.023
			75 cm	0.031	0.0020
1 Mbar	100 μ s	Lo-Pressure	10 cm	0.033	0.0069
			75 cm	0.031	0.0020
1 kbar	1 ns	Lo-Pressure	10 cm	0.50	0.137
			75 cm	0.41	0.037

* Listed values are peak pressures normalized by “driving” pressure.

... and attenuation for $p(t)$ -driven loading in water shows related features.

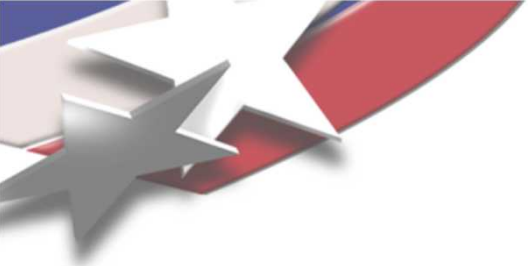
- Sample configuration:
 - > Inner “radii” of 10 cm and 5 cm;
 - > Buffer layer or liner of 1 cm of aluminum;
 - > Water layer of 80 cm.
- A pressure boundary condition, $p(t)$, is applied to the inner surface of the aluminum buffer. It is representative of pressure loads generated by Z.



Driving Pressure	Inner Radius	Equation of State	Lagrangian Position **	Slab Geometry * *	Cylindrical Geometry *
1 Mbar	10 cm	Lo-Pressure	10 cm	0.044	0.029
			75 cm	0.0084	0.0029
1 Mbar	5 cm	Lo-Pressure	10 cm	0.044	0.023
			75 cm	0.0083	0.0022

* Listed values are peak pressures normalized by “driving” pressure.

** Lagrangian positions are distances from inner material boundary.

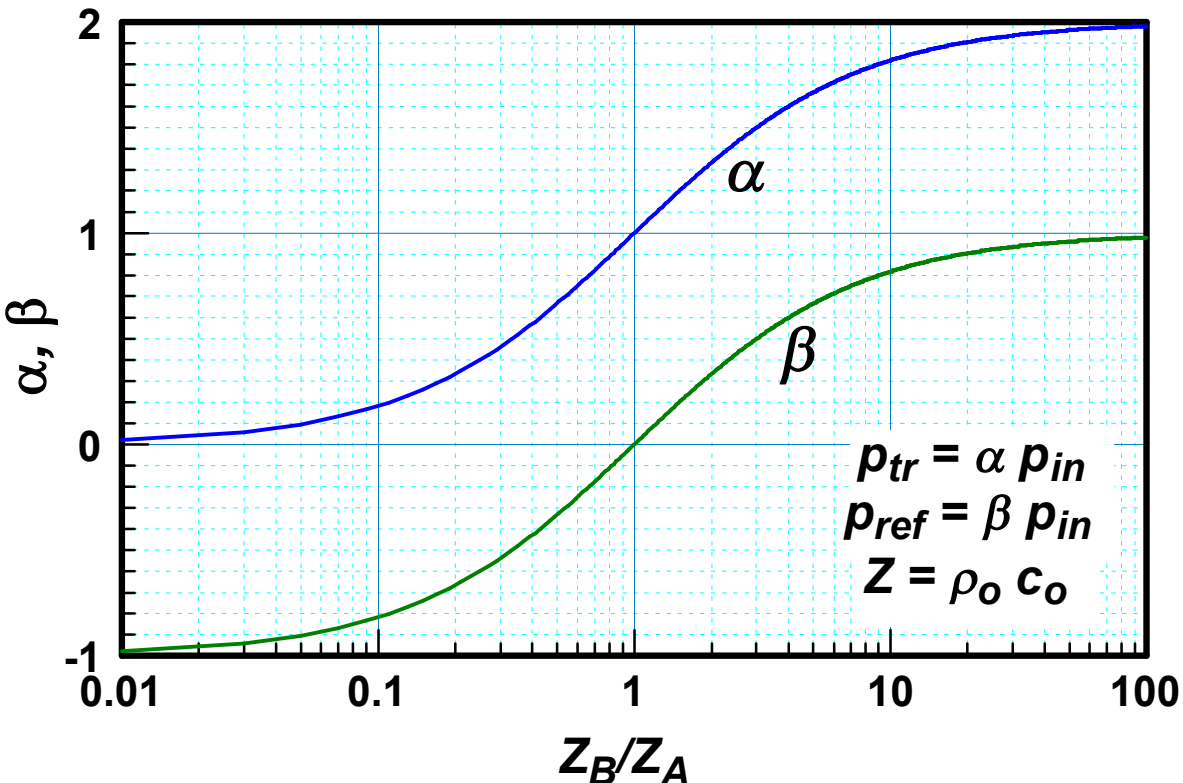


These attenuation calculations can be summarized in a simple fashion.

- Geometric (cylindrical) attenuation plays by far the largest role, but as starting (inner) radii become larger, the geometric effects are reduced. Note that as a rough estimate, shock attenuation due to geometric divergence can be separated from that due to material losses— $(1/r)^{1/2}$ for cylindrical, and $1/r$ for spherical.
- Reasonable variations in the water equation of state have a relatively small effect on shock attenuation.
- Pulse width can be important at short distances (early times); but less so for longer distances (later times); in particular for the source-region calculations.
- Greater loading levels increase the effects of EOS nonlinearities.
- Pressure transmission to surrounding containment materials can be determined through material impedances, independent of geometry.
- However, for many types of response, impulse (i.e., $\int p \cdot dt$ or $\int v \cdot dm$) may be more relevant than pressure.



Shock transmission and reflection at an interface is calculated from material impedances.



p_{in} — $p_{incident}$
 p_{tr} — $p_{transmitted}$
 p_{ref} — $p_{reflected}$

$$\alpha = 2(Z_B/Z_A)/(1 + (Z_B/Z_A))$$
$$\beta = \alpha - 1$$
$$p_{in} + p_{ref} = p_{tr}$$

For a shock wave traveling from mat'l A into mat'l B

Various Mat'l Impedances
[10^5 g/cm²·s]

$$Z_{\text{Water}} = 1.48$$

$$Z_{\text{FLIBE}} = 6.84$$

$$Z_{\text{Steel}} = 36.1$$

$$Z_{\text{Steel}}/Z_{\text{Water}} \approx 24$$

$$Z_{\text{Steel}}/Z_{\text{FLIBE}} \approx 5$$

For a potential IFE first-wall material, the properties for FLiBE have been reported.

Chemical Composition

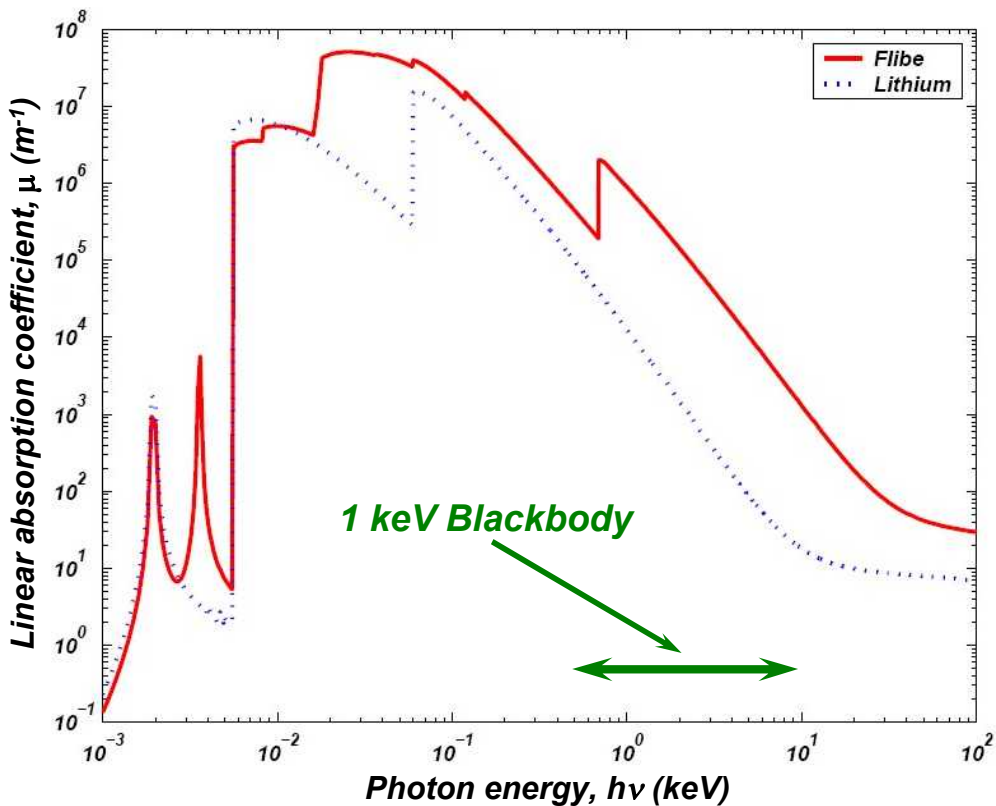
LiF – 67%; BeF₂ – 33%
Be – 6% ; Li – 18% ; F – 76%

Shock Properties

Density – $\rho_0 = 2 \text{ g/cm}^3$
Sound speed – $c_0 = 3.42 \text{ km/s}$
U_s/U_p slope – $s = 1.35$
Grüneisen parameter – $\gamma_0 = 0.96$

Thermal Properties

Specific sublimation energy – $\varepsilon_s \approx 1330 \text{ cal/g}$
Specific melt energy – $\varepsilon_m \approx 270 \text{ cal/g}$
Melt temperature – $T_m = 459 \text{ C}^\circ$
Specific heat – $C_v = 0.57 \text{ cal/g-K}$



– Zaghloul (2003)

A simple Mie Grüneisen EOS gives scaling laws for peak instantaneous pressure.

Simplified Mie Grüneisen EOS

$$p = \gamma_0 \rho_0 \varepsilon_{\text{surface}}$$

γ_0 – Grüneisen parameter

ρ_0 – density

$\varepsilon_{\text{surface}}$ – peak energy deposition

For FLIBE (1 keV):

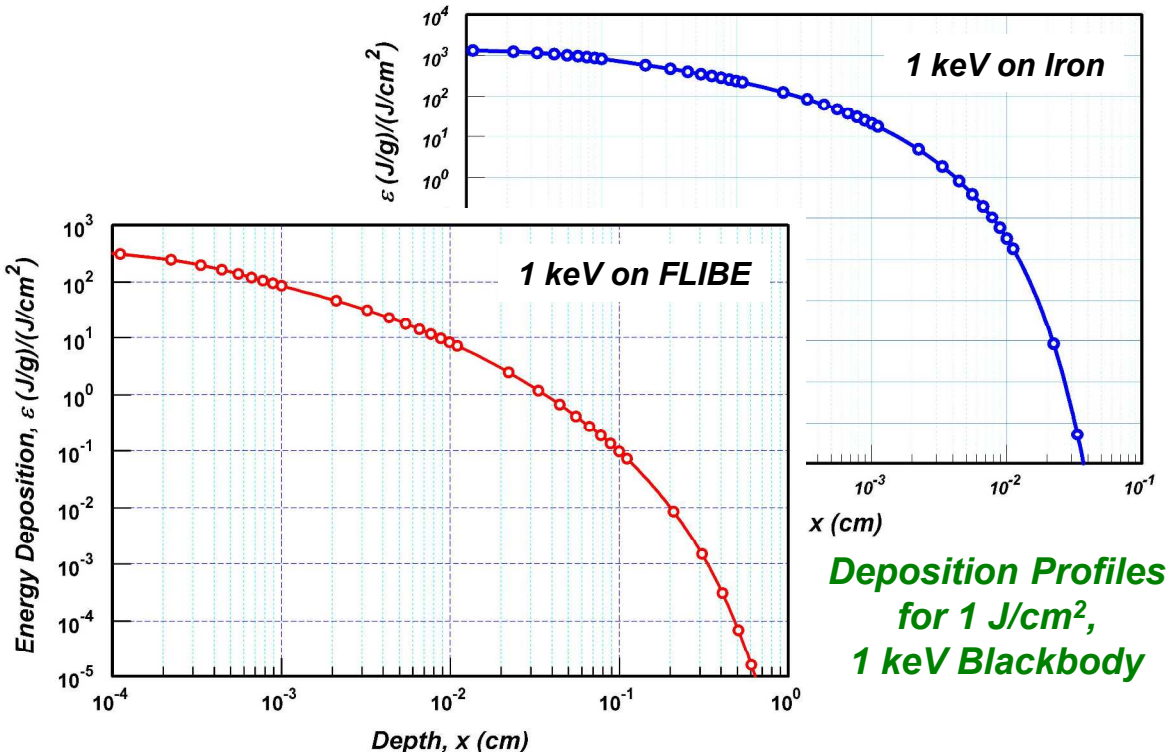
$$\varepsilon_{\text{surface}} \approx 400 \text{ (J/g)/(J/cm}^2)$$

$$p_{\text{peak}} \approx 0.8 \text{ GPa/(J/cm}^2)$$

For Steel (Iron) (1 keV):

$$\varepsilon_{\text{surface}} \approx 1400 \text{ (J/g)/(J/cm}^2)$$

$$p_{\text{peak}} \approx 22 \text{ GPa/(J/cm}^2)$$



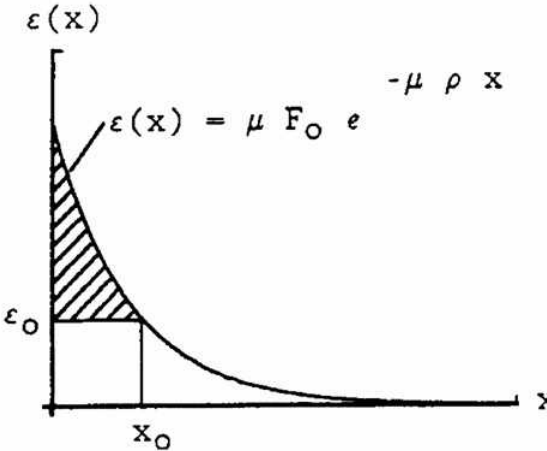
Scaling for Instantaneous Peak Pressure

$$p_{\text{peak}}(\text{FLIBE}) \approx 8 \text{ kbar/(J/cm}^2)$$

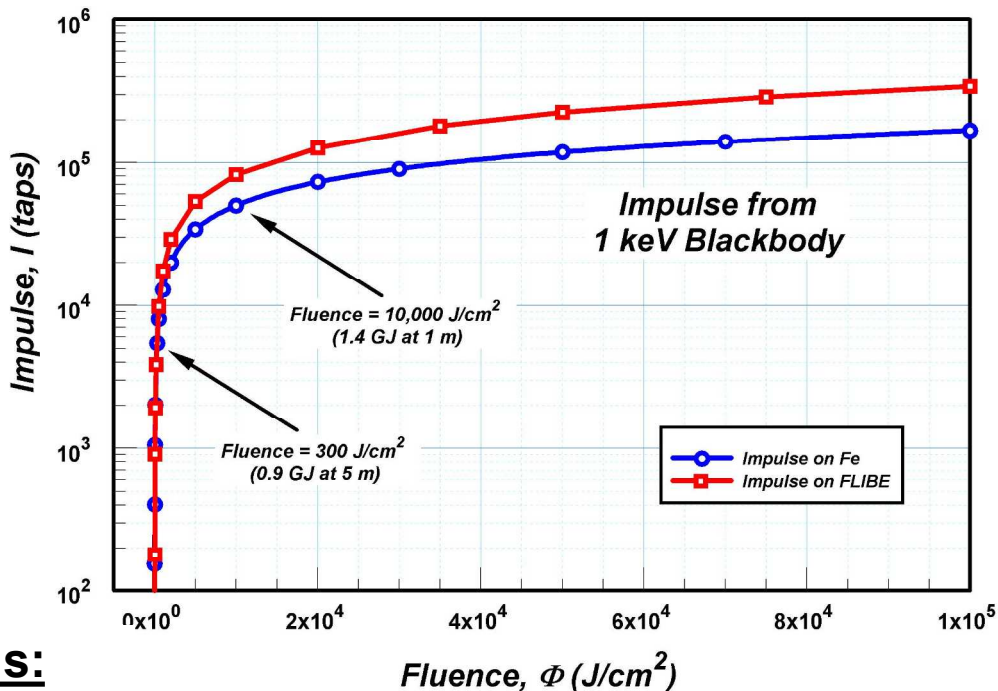
$$p_{\text{peak}}(\text{steel}) \approx 220 \text{ kbar/(J/cm}^2)$$

The modified BBAY model predicts dynamic impulse from simple energy deposition analyses.

MBBAY Model:



$$I = \alpha \sqrt{2} \left[\int_0^{x_0} \left\{ \mathcal{E}(x) - \mathcal{E}_0 \left(1 + \ln \frac{\mathcal{E}(x)}{\mathcal{E}_0} \right) \right\} \rho^2 x \, dx \right]^{1/2}$$



Typical Lethality Response Levels:

- Light-weight structure (e.g., satellite)
 > 1 to 10 ktaps *
- Medium-weight structure (e.g., airframe)
 > 10 to 30 ktaps
- Robust structure (e.g., RV)
 > 30 to 80 ktaps

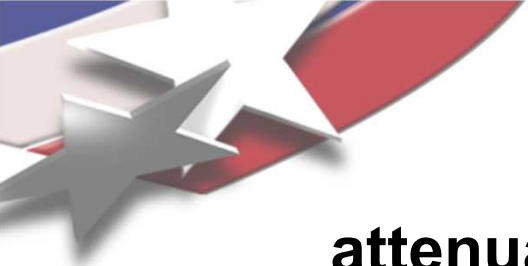
For FLIBE:

$I @ 10,000 \text{ J/cm}^2 - 82 \text{ ktaps}$

For steel (iron):

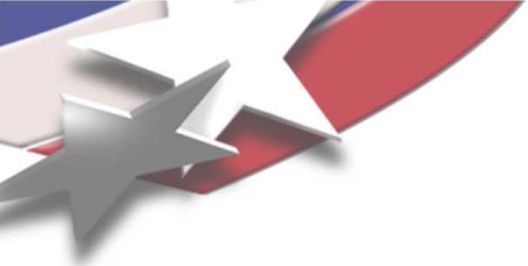
$I @ 300 \text{ J/cm}^2 - 5.5 \text{ ktaps}$





Simple models for peak shock pressure, attenuation, and impulse, have been described.

- We have demonstrated that IFE shock mitigation problems can be addressed with a combination of one-dimensional hydrodynamic calculations and simple analytic models.
 - > 1-D hydrocode calculations can rank important factors for shock attenuation, using planar, cylindrical, and spherical geometries.
 - > Simple shock physics provides the amplitudes of shocks crossing material interfaces.
 - > Along with energy deposition calculations, simplified Mie Grüneisen equations of state give scaling laws for peak instantaneous shock pressures.
 - > Analytic descriptions (MBBAY model) provide values for dynamic impulse (for structural response) in situations where pressures are at or below the material failure thresholds.
- These approaches are good for initial problem scoping and analysis of the relevant phenomenology. More elaborate multi-dimensional radiation-transport hydrocode will be needed for actual system designs.



References . . .

- M. E. KIPP and R. J. LAWRENCE, *WONDY V – A One-Dimensional Finite-Difference Wave Propagation Code*, SAND81-0930, Sandia National Laboratories, Albuquerque, NM (1982).
- N. B. MORLEY, “Compressible Response of Thin Liquid Film/Porous Substrate First Walls in IFE Reactors,” *Fusion Engineering and Design*, **42**, 563 (1988).
- R. J. LAWRENCE *et al.*, “The Response of Ceramic Powders to High-Level Quasi-Isentropic Dynamic Loads,” *Shock Compression of Condensed Matter—2003* (AIP CP706), M. D. Furnish *et al.*, Eds., American Institute of Physics, Melville, NY (2004).
- M. R. ZAGHLOUL *et al.*, “Thermo-Physical Properties and Equilibrium Vapor-Composition of Lithium Fluoride-Beryllium Fluoride (2LiF/BeF₂) Molten Salt,” *Fusion Science and Technology*, **44**, September (2003).
- R. LOWEN *et al.*, *XRAY Radiation Transport Program—User’s Handbook*, DNA-EH-92-12-G-V1, Defense Nuclear Agency, Alexandria, VA (1993).
- W. HERRMANN, “Constitutive Equation for the Dynamic Compaction of Ductile Porous Materials,” *J. Appl. Phys.*, **40** (6), 2490 (1969).
- D. L. McCLOSKEY and S. L. THOMPSON, *X-Ray-Induced Blowoff Phenomenology*, SC-DR-68-448, Sandia Laboratories, Albuquerque, NM (1969).